Quaternary Science Reviews 24 (2005) 2281–2300

Holocene fire and vegetation along environmental gradients in the Northern Rocky Mountains

Andrea Brunelle[a,*], Cathy Whitlock[b,1], Patrick Bartlein[b], Kurt Kipfmueller[c,2]

[a]Department of Geography, University of Utah, 260 S. Central Campus Dr. Rm. 270, Salt Lake City, UT 84112-9155, USA
[b]Department of Geography, University of Oregon, 1251 University of Oregon, Eugene, OR 97403-1251, USA
[c]Laboratory of Tree-Ring Research, University of Arizona, PO Box 210058, Tucson, Arizona 85721, USA

Received 6 February 2004; accepted 24 November 2004

Abstract

Holocene records of fire, vegetation, and climate were reconstructed from four sites in the Bitterroot Range region of the Northern Rocky Mountains in order to examine the vegetation and fire histories and evaluate the hypothesis proposed by Whitlock and Bartlein (1993) regarding the effects of increased summer insolation on precipitation patterns. Vegetation history in the series of sites was broadly similar. In the late-glacial period, the pollen data suggest open parkland dominated by *Picea* or alpine meadow, which reflect conditions cooler and drier than present. These open forests were replaced in the early to middle Holocene by forests composed mainly of *Pinus* and *Pseudotsuga*, which suggest conditions warmer than present. Modern forest compositions were in place by ca 3000 cal yr BP, and small variations in the timing of the vegetation shifts reflect local differences among sites. The long-term trends in fire occurrence support the hypothesis proposed by Whitlock and Bartlein (1993) that precipitation regimes were sharpened during the early Holocene summer insolation maximum but their location has remained unchanged as a result of topographic constraints. Sites located in areas currently summer-dry were drier-than-present during the early Holocene and fires were more frequent. Conversely, sites located in the areas that are summer-wet at present were wetter-than-present in the early Holocene, and fires were less frequent. On millennial time scales it appears that the climate boundary is controlled by topography and does not shift.

1. Introduction

The Holocene vegetation and climate history of the Northern Rocky Mountain region (NRM) is known from widely spaced paleoecological records in Idaho, Montana, and Yellowstone National Park (Mehringer et al., 1977; Karsian, 1995; Doerner and Carrara, 1999, 2001; Millspaugh et al., 2000; Brunelle and Whitlock, 2003; Millspaugh et al., 2004). This study examines the Holocene records from a series of sites in the Bitterroot Range along a precipitation gradient to study the variations in vegetation and fire history caused by changes in the distribution of insolation. The Bitterroot Range and nearby mountains of northern Idaho and western Montana are part of the NRM complex (Fig. 1). Extensive glaciation during the late Pleistocene is evidenced by the rugged peaks and deeply dissected valleys of the Bitterroot Range, which today creates steep environmental gradients. Sergeant Patrick Gass of the Lewis and Clark expedition described the Bitterroot Range as "the most terrible mountains I ever beheld" (Ronda, 1984), and Clark himself wrote from a mountain peak that "from this mountain I could observe high ruged [sic] mountains in every direction as far as I could See" (Moulton, 1988).

*Corresponding author. Tel.: +1 801 585 5729; fax: +1 801 581 8219.
E-mail address: andrea.brunelle@geog.utah.edu (A. Brunelle).
[1]Present address: Dept. of Earth Sciences, Montana State University, Bozeman, MT 59715.
[2]Present address: Dept. of Geography, University of Minnesota, Minneapolis, MN 55455.

0277-3791/$ - see front matter
doi:10.1016/j.quascirev.2004.11.010

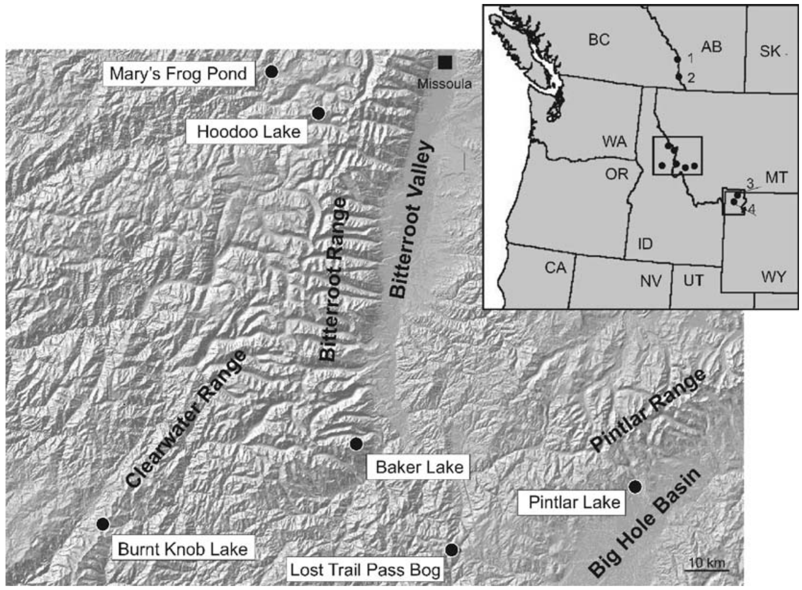

Fig. 1. Map showing the mountain ranges and physiographic features of the Bitterroot region of the NRM and the locations of sites discussed in the text on a 30 m DEM. Inset map shows other fire history sites in the NRM region. (1) Dog Lake (Hallett and Walker, 2000); (2) Bluebird Lake (Hebda, 1995); (3) Slough Creek Lake (Millspaugh and Whitlock, in press); (4) Cygnet Lake (Millspaugh et al., 2000).

These rugged landscapes are characterized by seasonal and spatial variations in climate that affect the distribution of plant communities. Most of the precipitation comes as winter snow produced by weather systems that form in the Gulf of Alaska and northeast Pacific Ocean (Finklin, 1983; Mock, 1996). These storms release moisture originally derived from the subtropical central and western Pacific Ocean, and, because of the elevation and north–south orientation of the Bitterroot Range, the west side of the Bitterroot Range receives nearly three times as much winter precipitation as the east side (Fig. 2) (Whitlock and Bartlein, 1993).

The mechanisms and sources of summer precipitation at present are variable, but they are generally associated with large-scale circulation features operating in the western United States. In the American Southwest, Great Plains, and eastern NRM, summer convective thunderstorms are triggered by surface heating and supported by upper-level disturbances. The moisture source for any resulting precipitation in these areas is the Gulf of Mexico and the Gulf of California. In the Pacific Northwest, large-scale subsidence associated with the eastern Pacific subtropical high-pressure system and the western North American ridge suppresses precipitation in summer. The resulting spatial pattern of the seasonality of precipitation displays a strong regional contrast (Tang and Reiter, 1984; Mock, 1996), inasmuch as the Pacific Northwest and western side of the NRM receive less summer precipitation relative to annual precipitation than does the eastern side of the NRM, Great Plains and Southwest (Fig. 2). These two precipitation regimes are evident in the Bitterroot region, with a slightly more summer-dry climate on the western side than on the eastern side.

Variations in the annual precipitation regime influence the elevation ranges of taxa in the Bitterroot region. On the west side of the Bitterroot crest, alpine tundra is present above elevations of 2500 m (Fig. 3) and *Larix lyallii* (alpine larch) and *Pinus albicaulis* (whitebark pine) dominate high-elevation parkland. Subalpine forest is present from 1700 to 2500 m elevation and characterized by *Larix lyallii*, *Pinus albicaulis*, *Picea engelmannii* (Engelmann spruce) and *Abies bifolia* (subalpine fir). Montane forest occurs from 1000 to 1700 m elevation, with *Pinus contorta* (lodgepole pine) and *Pseudotsuga menziesii* (Douglas-fir) as the dominant trees. Grassland and *Artemisia* (sagebrush) steppe are present below ca 1000 m elevation. On the east side of the Bitterroot Range and in the Pintlar Range to the southeast, vegetation zones similar to those on the west side are located at slightly higher elevations probably as a result of lower annual precipitation (Arno, 1979). On the east side, tundra occurs above ca 2750 m elevation, and subalpine forest and parkland range from ca 2100 to 2750 m elevation. The eastern montane forest is compressed to ca 1750–2100 m elevation with grassland and steppe below (Fig. 3). Botanical nomenclature follows Hitchcock and Cronquist (1973), except in the case of *A. bifolia*, which is distinguished from *Abies lasiocarpa* as a distinct species (Palmer and Parker, 1991; Hunt, 1993).

Over the past 21,000 years (i.e. the Last Glacial Maximum to present), several large-scale controls of climate have likely influenced the regional paleoclimatic

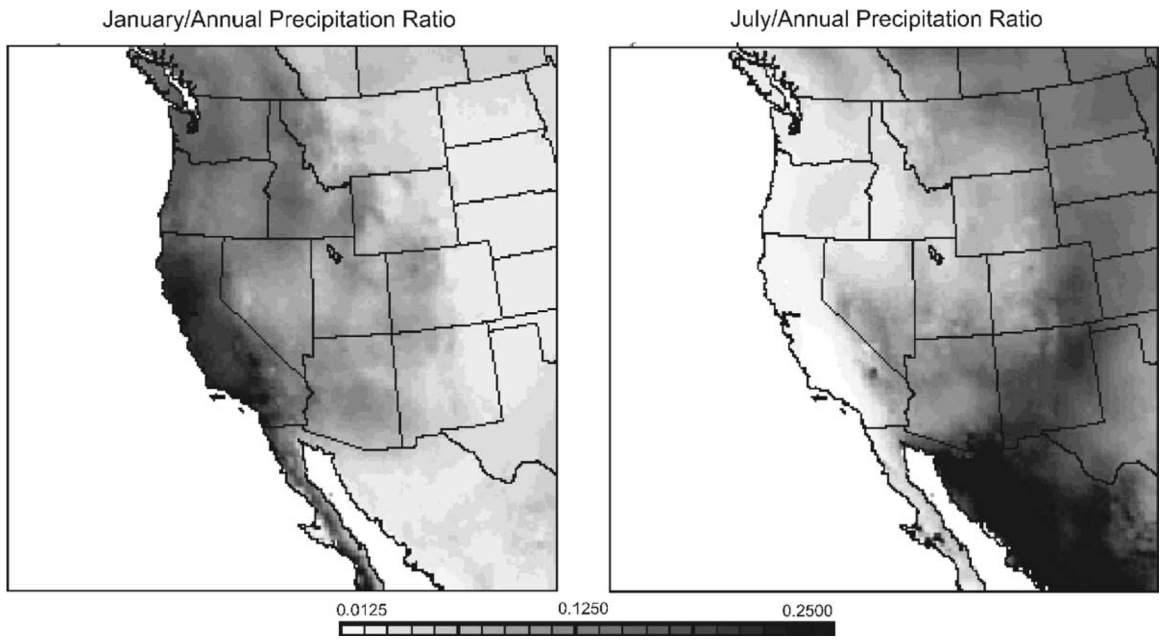

Fig. 2. Seasonal distribution of precipitation in the western United States based on ratios of January and July to annual precipitation. Darker areas indicate a high ratio, light areas indicate a low ratio. Notice that the Pacific Northwest, California, and western NRM receive the most precipitation in winter, whereas the southwestern United States, Great Plains, and western NRM receive more precipitation in summer (after Whitlock and Bartlein, 1993).

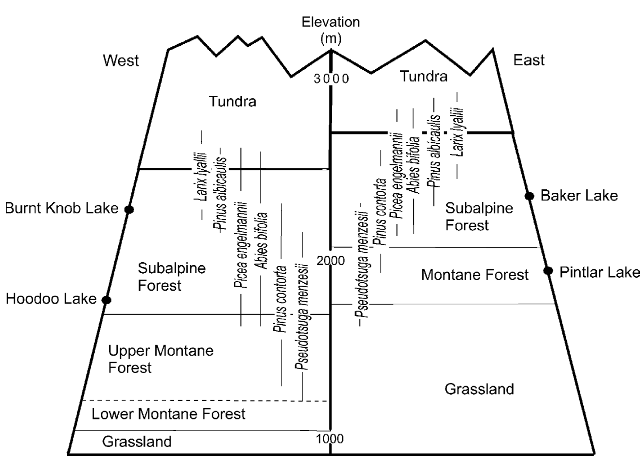

Fig. 3. Vegetation zones for the NRM of Idaho and Montana with the locations of the study sites based on Arno, 1979.

history of the NRM region. These controls include the area and height of the ice sheet, Pacific sea-surface temperatures, the seasonal cycle of insolation, and atmospheric composition. The regional impact of these controls on millennial time scales has been evaluated with sequences of paleoclimatic model simulations (Barnosky et al., 1987; Bartlein et al., 1998; Whitlock et al., 2001; Bartlein and Hostetler, 2004), and compared with syntheses of paleoenvironmental data (e.g. Thompson et al., 1993; Mock and Brunelle-Daines, 1999; Harrison et al., 2003) We use the large-scale features revealed by these analyses (Table 1, see also, e.g. Table 1 in Whitlock et al., 2001; Table 1 in Bartlein and Hostetler, 2004) to provide a context for interpreting the records in the NRM region.

The large-scale and long-term variations of climate governed by the changing controls are superimposed on spatial variations of climate that arise from the topographic complexity of the region and the temporal variations generated by interannual-to-millennial scale ocean–atmosphere interactions over the Pacific. Based on paleoecological research in Yellowstone National Park and the Wind River Range and consideration of those sequences of simulations, Whitlock and Bartlein (1993), Fall et al. (1995), and Millspaugh et al. (2004) proposed that the amplification of the seasonal cycle of insolation during the early Holocene sharpened the contrast between summer-wet and summer-dry precipitation regimes in the NRM compared to that at present. They also suggested that the spatial pattern of the precipitation regimes did not change during the Holocene because then, as at present, that pattern is related to large-scale physiography. Indeed, the spatial expression of these precipitation regimes has varied little during recent decades when the instrumental record can be used to compare years with anomalous atmospheric circulation patterns with long-term average circulation and surface-weather patterns (Mock, 1996). The present examination of the Holocene environmental history of the Bitterroot region is a further test of Whitlock and Bartlein's (1993) spatial heterogeneity hypothesis in the NRM region.

Table 1
Simulated climate for Late Glacial, Early Holocene, and Middle Holocene time periods based on CCM1 (Kutzbach et al., 1998)

	Late Glacial (16,000–11,000 cal yr BP) 14 ka simulation	Early Holocene (11,000–6800 cal yr BP) 11 ka simulation	Middle Holocene (6800–3500 cal yr BP) 6 ka simulation
Boundary conditions[a]	Ice 60% full glacial size CO_2 230 ppmv Insolation 6% higher in summer/6% lower in winter	Ice 30% full glacial size CO_2 267 ppmv Insolation 8% higher in summer/8% lower in winter	Ice near modern value CO_2 267 ppmv Insolation 6% higher in summer/6% lower in winter
Simulated climate responses:			
Hemisphere	Winter temperatures lower than present due to presence of glacial ice and decreased winter insolation[a,b] Summer temps higher than last glacial maximum (LGM) due to increasing summer insolation but similar to present[a,b]	Winters temperatures still slightly lower than modern[a,b] Summers warmer (2–4 °C) than LGM or present due to elevated summer insolation[a,b]	Winter temperatures similar to modern[a,b] Summers warmer (1–2 °C) than LGM or present due to elevated summer insolation[a,b]
Western US	Northeast Pacific subtropical high (STH) stronger than present (summer)[a,b] Deeper- than- present thermal low in southwest (summer)[a,b] Winter ppt: wetter higher than present[a,b] Summer ppt: drier lower than present[a,b]	STH stronger than previously or present (summer)[a,b] Thermal low deeper than previous or present in southwest (summer)[a,b] Winter ppt: drier lower than previous, similar to modern[a,b] Summer ppt: drier lower than previous or present[a,b] Less that previous effective moisture in Pacific Northwest, more in southwest[c]	STH weaker than previously, but still stronger than present (summer)[a,b] Thermal low weaker than previously, but stronger than modern in southwest (summer)[a,b] Winter ppt: wetter higher than previously or at present[a,b] Summer ppt: localized regions of wetter higher than previous or present, localized regions of drier lower than previous or present[b] Stronger monsoon activity in the southwest; Amplified Subtropical Ridge[c]
Summer-wet/summer-dry regions	Summer-dry: drier than present due to enhanced STH, and suppression of ppt[b] Summer-wet: wetter than present due to deeper than present thermal low and stronger than present onshore flow[b]	Summer-dry: summers drier than present or previously due to enhanced STH and suppression of ppt[b] Summer-wet: summers wetter than present or previously due to deeper-than-present thermal low and stronger than present onshore flow[b]	Summer-dry: summers drier than present but wetter than previous enhanced STH and suppression of ppt[b] Summer-wet: summers wetter than present but drier than previous due to deeper-than-present thermal low and stronger than present onshore flow[b]
Conceptual model for Bitterroot region	Summer-dry sites (west of Bitterroot crest) would be slightly drier than present; Summer-wet sites (east of Bitterroot crest) would be slightly wetter than present	Summer-dry sites (west of Bitterroot crest) would be drier than present; Summer-wet sites (east of Bitterroot crest) would be wetter than present	Summer-dry sites (west of Bitterroot crest) would be slightly drier than present; Summer-wet sites (east of Bitterroot crest) would be slightly wetter than present

Responses for the Northern Hemisphere, Western United States, and Summer-wet/Summer-dry regions are described as well as the implications for the Bitterroot Region.
[a]Kutzbach et al. (1998).
[b]Bartlein et al. (1998).
[c]Mock and Brunelle-Daines (1999).

Fossil pollen, plant macrofossils, and macroscopic charcoal were examined at four lakes in the Bitterroot region at the modern summer-wet/summer-dry boundary. The objectives were to (1) reconstruct the vegetation, fire, and climate history of the Bitterroot region and evaluate the response of vegetation and fire regimes to changes in the large-scale climate controls that occurred on millennial time scales, and (2) use the fire history information as a proxy of summer precipitation to test the Whitlock and Bartlein (1993) hypothesis.

1.1. Site descriptions

The sites lie in montane and subalpine forests along a west-to-east gradient of increasing summer-to-annual precipitation (Table 2). Burnt Knob Lake (45.704°N,

Table 2
Physical and climatic data for the study sites

	WEST Burnt Knob	Hoodoo	Baker	EAST Pintlar Lake
Elevation (m)	2250	1770	2300	1921
Latitude	45.704444	49.320556	45.891944	45.840556
Longitude	−114.98667	−114.650278	−114.26194	−113.44028
Modern forest type	Subalpine	Subalpine	Subalpine	Montane
Recent fire years	1883, 1709/1719/1729 complex, 1580, 1527	1889	1896, 1748, 1204	na
Origin of basin	Cirque	Cut-off stream channel	Cirque	Glacial valley
Avg. Jan temp (°C)[a]	−10.1	−4.7	−10.3	−8.5
Avg. July temp (°C)[a]	10.8	18.1	11	14.9
Avg. Jan ppt (mm)[a]	182	169	100	59
Avg. July ppt (mm)[a]	35	38	31	35
Jan/annual ppt[a]	0.1438	0.1421	0.1253	0.0964
Jul/annual ppt[a]	0.0276	0.032	0.0388	0.0572

[a]Elevationally adjusted interpolations of nearby weather station data (Bartlein, unpublished data, 2001).

114.987°W, elevation 2250 m) is located in a cirque basin on the western side of the Bitterroot Range in an open subalpine forest dominated by *A. bifolia*, *P. albicaulis*, and *P. contorta. P. engelmannii* is also present in the watershed. *Alnus viridis* (green alder) and *Salix* spp. (willow) grow in moister areas. Dominant understory species include *Vaccinium scoparium* (whortleberry), *Xerophyllum tenax* (beargrass), and *Phyllodoce empetriformis* (mountain heather). Various members of Poaceae (grass family), Asteraceae (sunflower family), and Rosaceae (rose family) are also present.

Hoodoo Lake (49.321°N, 114.650°W, elevation 1770 m), is located on the local summit of the Bitterroot Range (Fig. 1), and occupies a cutoff stream channel formed at ca 12,000 cal yr BP. The subalpine forest at Hoodoo Lake is dominated by *P. contorta. P. engelmannii. A. bifolia* is also present in the watershed, mainly on the wet slopes near the lake. *Salix* and *Scirpus* (sedge) are present around the lake margin. Dominant understory species include *V. scoparium*, *X. tenax*, and *P. empetriformis*. Various members of Poaceae and Asteraceae are also present in the watershed.

Baker Lake (45.892°N, 114.262°W, elevation 2300 m) is on the east side of the Bitterroot Range in a late-Pleistocene cirque basin (Fig. 1). *P. albicaulis* and *L. lyallii* grow on dry slopes, and *A. bifolia* and *P. engelmannii* occur in wetter locations within the basin. *P. contorta* is also present. Dominant understory species include *V. scoparium*, *V. membranaceum* (huckleberry), *X. tenax*, and *P. empetriformis*.

Pintlar Lake (45.841°N, 113.440°W, elevation 1921 m) is in the Pintlar Range in a valley draining into the Big Hole Basin. Pintlar Lake is dammed behind a late-Pleistocene end moraine and lies in montane forest of *P. contorta* with *P. menziesii* and *P. engelmannii* as minor components. Dominant understory species include *Arctostaphylos uva-ursi* (kinnikinnick), *Artemisia tridentata* (big sagebrush), *Linnea borealis* (twinflower) and *Ribes* spp. (gooseberry).

2. Methods

All lakes were cored from a platform anchored in the center of the lake. The uppermost unconsolidated sediments were collected (except at Pintlar Lake) with a plastic tube outfitted with a piston, and sampled in the field in 1-cm increments. Long cores were obtained using a modified Livingstone corer. Each drive was extruded and wrapped in plastic wrap and aluminum foil in the field and stored under refrigeration in the lab. The long and short cores from Burnt Knob, Baker, and Hoodoo lakes were correlated by the presence of distinctive charcoal peaks.

Cores were split lengthwise, and color and lithology were described. One cubic centimeter samples were taken every 5 cm from the short cores, and at 10-cm intervals for the long cores to calculate water, organic, and carbonate contents. Samples were dried for 24 h at 60 °C to measure water content. Organic and carbonate contents were determined by weight loss after the samples were ignited for 2 h at 550 ° and 900 °C, respectively (Dean, 1974).

Magnetic susceptibility was measured to identify intervals with high levels of ferromagnetic minerals. These intervals are associated with runoff from adjacent slopes or from deposition of volcanic ash (Thompson and Oldfield, 1986; Gedye and Oldfield, 2000). Samples of 8-cm^3 volume were taken in contiguous 1-cm intervals from the short and long cores and placed in plastic vials. Magnetic susceptibility was recorded in electromagnetic units (emu) with a Sapphire Instruments cup-coil sensor.

Five cubic centimeter samples were taken from the long and short cores at contiguous 1-cm intervals for charcoal analysis. The samples were soaked in sodium hexametaphosphate to disaggregate the sediment, which was then washed through >125 and >250 μm mesh sieves. These sizes were chosen because modern studies have shown that large charcoal particles do not travel far from their source (Clark, 1988; Whitlock and Millspaugh, 1996; Gardner and Whitlock, 2001), and our objective was to reconstruct local fire history. The sieved material was counted separately under a dissecting microscope at 20–32× magnifications for ease of counting and to look for trends in the individual size classes, and then the totals of the two size fractions were combined.

The charcoal analysis methods follow those described in Long et al. (1998) and have been applied to records from several sites in North America to reconstruct long-term fire histories (e.g., Hallett and Walker, 2000; Millspaugh et al., 2000; Mohr et al., 2000; Brunelle and Anderson, 2003). The charcoal counts were divided by the volume of sediment sampled to calculate charcoal concentrations (particles/cm^3). Concentrations were interpolated to pseudo-annual values and then binned in 8–30 year time intervals to preserve the highest resolution of the record. For example, the minimum deposition time for 1 cm of sediment at Baker Lake was 25 years, so this interval was chosen as the bin width for that site (see Long et al. (1998), Whitlock and Larsen (2002) for a more detailed explanation). Bin-width values for the other sites include 8 years at Pintlar Lake, 30 years at Burnt Knob Lake, and 10 years at Hoodoo Lake. Charcoal accumulation rates (CHAR) (charcoal particles/cm^2/yr) were obtained by dividing the charcoal concentration for each bin (particles/cm^3) by the deposition time (yr/cm). To identify fire episodes, CHAR was separated into two components. The background component represents trends in charcoal production and deposition, and the peaks component consists of charcoal values above background that register fire episodes. The background component reflects changes in vegetation, surficial transport to the lake, and sediment deposition within the lake itself (Bradbury, 1996; Whitlock and Millspaugh, 1996). The background component is represented by a locally weighted average (see Cleveland (1993) for discussion), the smoothness of which is controlled by the width of the (local) weight function (or "window width"). A fire episode (defined in Brunelle and Whitlock, 2003) is identified when CHAR exceeded background by a prescribed threshold ratio.

These two parameters interact: an overly large window width ("underfitting" the background component) or a low threshold parameter may result in many small peaks, while a window width that is too small (overfitting the background component) or a threshold ratio that is too large may miss peaks. In practice, a range of values for the background window width is examined to select a value that adequately describes the slow variations in charcoal influx while avoiding "undue wiggles" in the background component (Cleveland, 1993, p. 98). Next, a range of threshold-ratio values is examined, and the ages of the individual peaks are compared with the ages of known fires or with modern fire return intervals. The frequency of charcoal peaks or fire episodes is summarized by determining the locally weighted average-frequency of peaks (expressed as the number of peaks per 1000 yr).

During the past several hundred years, fires were identified using dendrochronological techniques. Widespread fires were identified by three criteria in the tree-ring record: (1) the fire scar data were supported by stand-age data (e.g. a post-fire recruitment pulse): (2) the fire year was identified by two or more trees separated from each other by at least 500 m; and (3), snag or survivor germination dates in a stand of more recent origin fell within 20 years of a known fire event determined by the above criteria. Local fires were defined by two criteria: (1) fire events were recorded as a single fire scar or group of scars on trees within 500 m, and (2) there were no supporting stand age data to suggest a large event (Kipfmueller, 2003). These designations assured a conservative estimate of widespread fires. Independent information on past fires was not available for the Pintlar Lake watershed.

Pollen samples were taken every 10 cm (at ca 100–400 year intervals) in both long and short cores and processed following the methods of Faegri et al. (1989). *Lycopodium* was added to each sample as an exotic tracer. Pollen grains were identified at 500× magnification to the lowest possible taxonomic level with the University of Oregon pollen reference collection and published atlases (e.g. Kapp, 1969; Moore et al., 1991). At least 300 terrestrial grains were counted per sample, and counts were converted to percentages of total terrestrial grains. Pollen accumulation rates (PAR; grains/cm^2/yr) were calculated by dividing pollen concentrations (grains/cm^3) by the deposition time (yr/cm) to identify changes in abundance of individual taxa over the record.

Diploxylon- and haploxylon-type *Pinus* grains were assigned to *P. contorta* and *P. albicaulis* based on the presence or absence of verrucae on the distal membrane (Moore et al., 1991). Both species grow in the region and the presence of needle fragments in the cores confirmed the assignments. However, the possibility that *P. ponderosa* contributed to the Diploxylon-type *Pinus* pollen, and that *Pinus monticola* and *Pinus flexilis* pollen were components of the Haploxylon-type *Pinus* cannot be dismissed, because these conifers grow in this part of the NRM. Grains lacking distal membranes were identified as *Pinus* undifferentiated. *Abies* pollen was referred to *A. bifolia*, and *Picea* pollen was assigned to *P. engelmannii*, based on the macrofossil identifications.

Pseudotsuga and *Larix* pollen grains are indistinguishable (Moore et al., 1991) and labeled as *Pseudotsuga*/*Larix* on the pollen diagrams. However, in the discussion of each site, the genus designation (either *Pseudotsuga* or *Larix*) is based on which conifer grows nearest to the site or is suggested by the presence of macrofossils. Pollen grains that could not be identified with available reference material were classified as "Unknown." Pollen grains that were hidden or degraded were classified as "Indeterminate."

Needle and male cone remains in the core were identified from the sieved residues using the modern reference collection at the University of Oregon and reference material from the Oregon State University Herbarium. The presence of needle and male cone macrofossils was noted on the pollen percentage diagram.

Paleoclimate model simulations provide independent information on the likely regional responses to large-scale changes in the climate system. In this study, we used results from a sequence of simulations by Kutzbach et al. (1998) using the NCAR (National Center for Atmospheric Research) CCM 1 (Community Climate Model) as described by Bartlein et al. (1998). CCM 1 is an atmospheric general circulation model (AGCM) with a "mixed-layer" ocean that can simulate the sea-surface temperature response to altered wind and radiation forcing, but not the ocean-circulation response.

In this sequence of simulations, insolation levels, ice-sheet size, and atmospheric carbon-dioxide concentrations were varied in a realistic fashion, and although the resolution of the model is quite coarse relative to the network of sites being discussed here, the implications of the large-scale atmospheric circulation variations and surface energy- and water-balance for the NRM can still be inferred (see Bartlein et al. (1998) for discussion). The 14,000, 11,000, and 6000 yr BP simulations represent late-glacial, early Holocene, and mid-Holocene conditions, respectively. The late Holocene was not part of the model experiments.

3. Results

3.1. Lithology

The sedimentary record at all sites was generally similar in lithology and length, with the exception of Pintlar Lake, which had approximately twice the sediment recovery of the others. Burnt Knob, Baker, and Pintlar lakes had basal sediments consisting of inorganic clay and silt (organic content $<5\%$) that were probably deposited in an oligotrophic lake. Magnetic susceptibility data were not available for Pintlar Lake; however, at Burnt Knob and Baker lakes, the values were relatively high (ca $10\,\text{emu} \times 10^{-5}$) in this lowermost unit (Fig. 4) suggesting rapid deposition of minerogenic sediment during deglaciation. The inorganic clay was overlain by fine detritus gyttja (10–30% organic content) suggesting a shift to a more productive lake and less terrestrial input. At Hoodoo Lake, the basal sediments began with well-sorted gravel that graded upward to sand and silt. Fine detritus gyttja also overlaid the silt deposit at Hoodoo Lake marking the initiation of a closed lake system. Both magnetic susceptibility and the organic content remained fairly constant in most of the Hoodoo Lake record, suggesting little change in terrestrial input to the lake. All sites recorded low organic content and high magnetic susceptibility in association with volcanic ash deposits. Tephra samples from Burnt Knob Lake and Baker Lake were identified as Mazama and Glacier Peak ashes based on electron microprobe and chemical analyses (A. Sarna-Wojcicki, unpublished data, 2001). Depth, thickness, and texture of the ash layers at Hoodoo and Pintlar lakes suggested similar sources.

3.2. Chronology

Age models for the Bitterroot records were developed from AMS-^{14}C age determinations, ^{210}Pb dates (Table 3), and the age of Mazama (7627 cal yr BP, Zdanowicz et al., 1999) and Glacier Peak ashes (13,155 cal yr BP, Carrara and Trimble, 1992). A series of ^{210}Pb dates in the short cores provided sedimentation rates (cm/yr) for the last ca 150 years. Radiocarbon dates were converted to calendar years before present (cal yr BP) using CALIB 4.1 (Stuiver et al., 1998). Age-versus-depth relations were based on a series of polynomial regressions (Table 3).

At Burnt Knob Lake, distinctive charcoal peaks matched known fires in A.D. 1883, 1709/1719/1729, 1580, and 1527 based on tree-ring records (Kipfmueller, 2003). These fire years were included in the depth-age model at Burnt Knob Lake (Brunelle and Whitlock, 2003; Kipfmueller, 2003). Three fires were identified from tree-ring records in the Hoodoo Lake watershed in A.D. 1934, 1889, and 1851 and three fires occurred in the Baker Lake watershed in A.D. 1896, 1748, and 1204 that were used in the age models for those sites (Kipfmueller, 2003). A summary of the tree-ring fire records for Burnt Knob, Baker, and Hoodoo Lakes can be found in Fig. 5.

3.3. Macroscopic charcoal record

In the decomposition of the CHAR time series, a range of background window-width and peak threshold-ratio parameter values was considered (Brunelle-Daines, 2002). A background window-width of 750 years adequately fit the slow variations in CHAR at subalpine sites (Burnt Knob, Hoodoo, and Baker lakes), whereas a

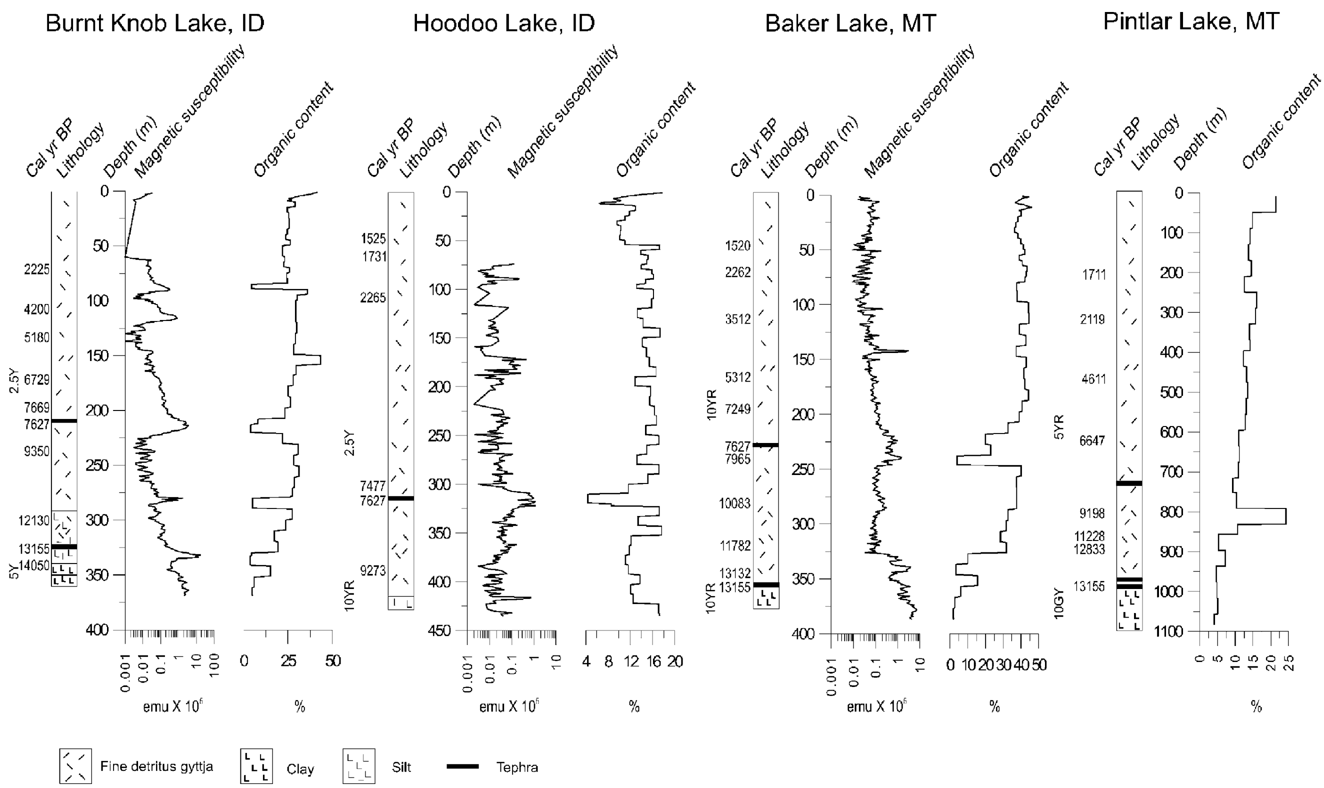

Fig. 4. Lithology, magnetic susceptibility, and organic content for the study sites (arranged from west to east). Lithologic symbols after Troels-Smith (1955), and Munsell color descriptions to the left of the lithologic column (Goddard et al., 1984). Magnetic susceptibility data are not available for Pintlar Lake.

600-year window was applied to the CHAR record from the montane-forest site, Pintlar Lake (Fig. 6). Threshold ratios ranged from 1.15 to 1.30 with the final selection based on the best match between the ages of charcoal peaks and known fires and a reconstructed fire-return interval for the last 1000 years that matched closely with modern ecological data on fire frequency.

At Baker and Pintlar lakes, background charcoal levels were low initially, then increased at ca 12,000 cal yr BP and remained essentially constant for the rest of the record (Fig. 6). Values at Hoodoo Lake showed little change, except for increasing slightly towards present. Background charcoal levels at Burnt Knob Lake were low before ca 14,000 cal yr BP, then increased and fluctuated throughout the Holocene. The variations in background levels in the Holocene probably represent changes in charcoal delivery from the lake basin, because they are not associated with changes in the vegetation inferred from the pollen record (see below).

Burnt Knob Lake recorded low fire frequencies (~three episodes/1000 years) during the late-glacial period. At about 12,000 cal yr BP fire frequency increased to five episodes/1000 years and remained high until ca 8000 cal yr BP. After 8000 cal yr BP, fire frequencies decreased to ~four episodes/1000 years where it remained essentially constant for the rest of the Holocene (Brunelle and Whitlock, 2003). Hoodoo Lake recorded moderate fire frequencies between ca 12,000 and 6000 cal yr BP (~four episodes/1000 years). Fire frequency was high (~six episodes/1000 years) from 6000 to 2000 cal yr BP, decreased to two episodes/1000 years at ca 2000 cal yr BP, and increased to almost four episodes/1000 years in the last few hundred years.

Baker Lake and Pintlar Lake showed similar patterns. Prior to ca 11,000 cal yr BP, both sites recorded relatively high fire frequencies (three and 12 episodes/1000 years, respectively), which after 11,000 cal yr BP, decreased to two episodes/1000 years at Baker Lake and four episodes/1000 years at Pintlar Lake. At both sites, fire frequency remained low until ca 6000 cal yr BP, when four and 10 episodes/1000 years were registered (respectively). After 6000 cal yr BP, the fire frequency at Baker Lake decreased (two episodes/1000 years) until ca 3000 cal yr BP, when it increased to modern levels (~four episodes/1000 years). At Pintlar Lake, fire frequency steadily increased from 8 episodes/1000 years at ca 6000 cal yr BP to 10 episodes/1000 years at present. Baker, Pintlar, and Hoodoo lakes recorded a period of high fire frequency centered at ca 2000 cal yr BP (Fig. 6).

Table 3
Uncalibrated and calibrated age determinations for study sites with age model regression equations

Depth (cm)	Lab number[a]	Material/source	Age	Age
			(^{14}C yr BP)	(cal yr BP)[b]
Burnt Knob Lake	$y = -1E-06x^2 + 0.023x^2 + 32.403x$			$R^2 = 0.9951$
0				−47
8		1883 fire		67
23		1709/1719/1729 fire		231
32		1580 fire		371
39		1527 fire		423
70.5	AA-27849	Conifer needles	2220±45	2336–2126 (2225)
104.5	AA-31755	Charcoal	3795±80	4413–3975 (4200)
135.5	AA-27847	Twig/charcoal	4485±50	5306–4966 (5180)
181	AA-27848	Male cone	5915±55	6880–6628 (6729)
207	AA-31756	Charcoal	6830±95	7857–7554 (7669)
213		Mazama ash		7627±150 (7627)[c]
240	AA-29546	Conifer needles	8300±100	9487–9062 (9350)
314	AA-29547	Conifer needles	10270±80	12389–11635 (12130)
332		Glacier Peak ash	11200[d]	13425–12997 (13155)
340	AA-32532	Conifer needles	11922±83	14140–13580 (14050)
Hoodoo Lake	0–50 cm : $y = 0.0235x^2 + 3.27x - 47$			$R^2 = 0.9825$
	50–400 cm : $y = -5E-05x^3 + 0.0786x^2 - 1.0051x + 1418.7$			$R^2 = 0.9984$
0				−47
16		1934 fire		16
30		1889 fire		61
34		1851 fire		99
49.5	AA-34825	Charcoal	1620±40	1574–1411 (1525)
64.5	AA-34826	Charcoal/wood	1825±40	1839–1690 (1731)
113.5	AA-35509	Needle/male cone	2245±35	2274–2154 (2265)
313.5	AA-35510	Conifer needle	6595±85	7614–7320 (7477)
322		Mazama ash		7627±150 (7627)[c]
400	AA-35511	Male cone/charcoal	8270±160	9544–8927 (9273)
Baker Lake	$y = 0.0226x^2 + 28.31x$			$R^2 = 0.9977$
0				−47
12		1896 fire		54
20		1748 fire		202
28		1204 fire		746
55	AA-34823	Conifer needles	1600±40	1568–1405 (1520)
75	AA-38087	Male cone	2209±49	2341–2111 (2262)
120	AA-38088	Conifer needles	3306±67	3644–3385 (3512)
169	AA-38089	Wood	4617±51	5472–5262 (5316)
207	AA-38090	Needles/seeds/wood	6302±55	7325–7154 (7249)
222		Mazama ash		7627±150 (7627)[c]
246	AA-38091	Needles/wood	7164±74	8113–7834 (7965)
289	AA-38092	Male cone/seeds	8870±120	10217–9625 (10083)
330	AA-38093	Male cone/needles/wood	10239±79	12375–11553 (11782)
362	AA-36943	Needles	11100±130	13441–12855 (13132)
375		Glacier Peak tephra	11200[d]	13425–12997 (13155)
Pintlar Lake	$y = -7.211x^4 + 131.57x^3 - 625.35x^2 + 1671.1x + 39$			$R^2 = 0.9873$
1.65	WIS-2175	Bulk sediment	1795±50	(1711)
3.25	WIS-2177	Bulk sediment	2130±160	(2119)
4.51	WIS-2178	Bulk sediment	4120±60	(4611)
6.08	WIS-2179	Bulk sediment	5830±70	(6647)
7.47	WIS-2180	Bulk sediment	8220±80	(9198)
8.07	WIS-2181	Bulk sediment	9860±90	(11228)
8.27	WIS-2182	Bulk sediment	10690±100	(12883)
9.32		Glacier Peak	11200[d]	(13155)

[a]Lab numbers refer to University of Arizona AMS Laboratory (AA-), and the University of Wisconsin-Madison (WIS-).
[b]CALIB 4.1 (Stuiver et al., 1998).
[c]Zdanowicz et al. (1999).
[d]Carrara and Trimble (1992).

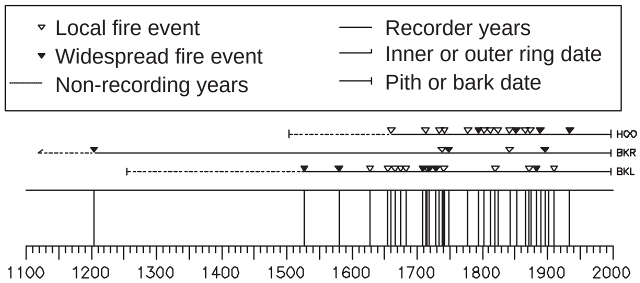

Fig. 5. Selway-Bitterroot three site composite fire chronology determined from tree rings from many trees at a site. Open triangles depict local fires and filled triangles widespread fires. Vertical lines at the bottom of the figure show all fires recorded in the three sites combined. Solid vertical lines show widespread fires occurring in any site and dashed vertical lines localized fires recorded in any site. Detailed treatment of tree-ring fire history methods can be found in Kipfmueller (2003).

3.4. Pollen record

The pollen records indicated broadly similar shifts in vegetation through time (Fig. 7). Prior to ca 13,000 cal yr BP the records featured pollen assemblages that suggested *Picea* parkland, a depressed upper treeline, and cool conditions. This vegetation type was best developed at Burnt Knob Lake where *Picea* percentages reached nearly 10% and *Artemisia* values exceeded 40%. *Picea* was less important at Baker Lake where *Pinus* was the dominant tree. The fact that there were few conifer macrofossils in the cores prior to ca 13,000 cal yr BP is consistent with open parkland conditions.

After ca 13,000 cal yr BP the vegetation shifted to closed pine forest, as evidenced by decreasing percentages of *Picea*, *Artemisia* and Poaceae pollen, increasing percentages of *Pinus* and *Abies* pollen, and the occurrence of abundant conifer macrofossils (Fig. 7). This shift from *Picea* parkland to *Pinus* forest suggests a rise in treeline due to warmer conditions than before. The transition occurred first at Burnt Knob and Pintlar Lake at ca 14,000 cal yr BP, then at Baker Lake at ca 12,500 cal yr BP, which may reflect the elevational gradient among the sites.

In the early Holocene, thermophilous taxa became more abundant at all sites suggesting further rise of treeline and continued warming. This transition occurred at Pintlar Lake at ca 11,000 cal yr BP and was marked by increasing percentages of *Pseudotsuga/Larix* type, *Alnus*, and *Salix* pollen and declining percentages of *Pinus* pollen. *Pseudotsuga/Larix* type pollen was abundant at Hoodoo Lake from ca 11,500 to ca 7500 cal yr BP. At Baker Lake, the transition to warm conditions occurred at ca 11,000 cal yr BP and was marked by a shift to high percentages of *Pseudotsuga/Larix* type, *Alnus*, and *Abies* pollen. Burnt Knob Lake showed increased percentages of *Pseudotsuga/Larix* type pollen after 10,000 cal yr BP, along with a rise in those of *Alnus*. After ca 13,000 cal yr BP, abundant macrofossils of *P. contorta* and *P. albicaulis* at Burnt Knob and Baker lakes support the interpretation of closed *Pinus*-dominated forests (Fig. 7) with a *Pseudotsuga/Larix* component.

In the late Holocene, the pollen data record the development of modern forest conditions and the onset of cooler, moister conditions. This transition occurred first at Burnt Knob Lake (ca 4000 cal yr BP) with increases in *P. contorta* and *P. albicaulis* pollen percentages at the expense of *Pseudotsuga/Larix*. Baker Lake registered this shift at ca 3500 cal yr BP when it was marked by decreased *Alnus* and increased *Abies* percentages. At Pintlar Lake, the shift occurred at ca 2500 cal yr BP and was marked by increased percentages of *P. contorta*. The transition to modern forest assemblages occurred last at Hoodoo Lake, at ca 2000 cal yr BP, and was evidenced by lower percentages of *Abies* and higher percentages of *Pinus* pollen than before. Needles of *Picea*, *Abies*, *P. albicaulis*, and *Larix* were abundant at Baker Lake after 12,000 cal yr BP however, they were generally absent at Burnt Knob and Hoodoo lakes after ca 2000 cal yr BP (Fig. 7). This abundance of conifer macrofossils at Baker Lake may be related to its rocky watershed, which would have facilitated the surface transport of forest litter to the lake.

4. Discussion

4.1. Vegetation, fire, and climate history of the Bitterroot region

Pollen records are available from a network of sites in the northwestern US that help disclose that nature of large-scale climate changes during the Holocene (see Barnosky et al., 1987; Thompson et al., 1993). Long-term fire reconstructions of the region are provided from a number of high-resolution charcoal records (see Whitlock et al., 2003), and these data show regional variations in fire occurrence related to changes in climate, as well as differences in elevation and forest type among sites. These two data sets provide a context for interpreting the environmental history of the Bitterroot region. In addition to the four sites in this study, records of long-term vegetation and fire history in the Bitterroot region have been described at Lost Trail Pass Bog and Mary's Frog Pond. Lost Trail Pass Bog (45.695°N, 113.948°W; 2147 m elevation) lies in forest dominated by *P. engelmannii*, *A. bifolia*, and *P. contorta* at the southern end of the Bitterroot Range in the summer-wet area (Mehringer et al., 1977). Mary's Frog Pond (46.637°N, 114.579°W; 2152 m elevation) is located in *A. bifolia* and *P. contorta* forest west of the Bitterroot crest in the summer-dry area (Karsian, 1995).

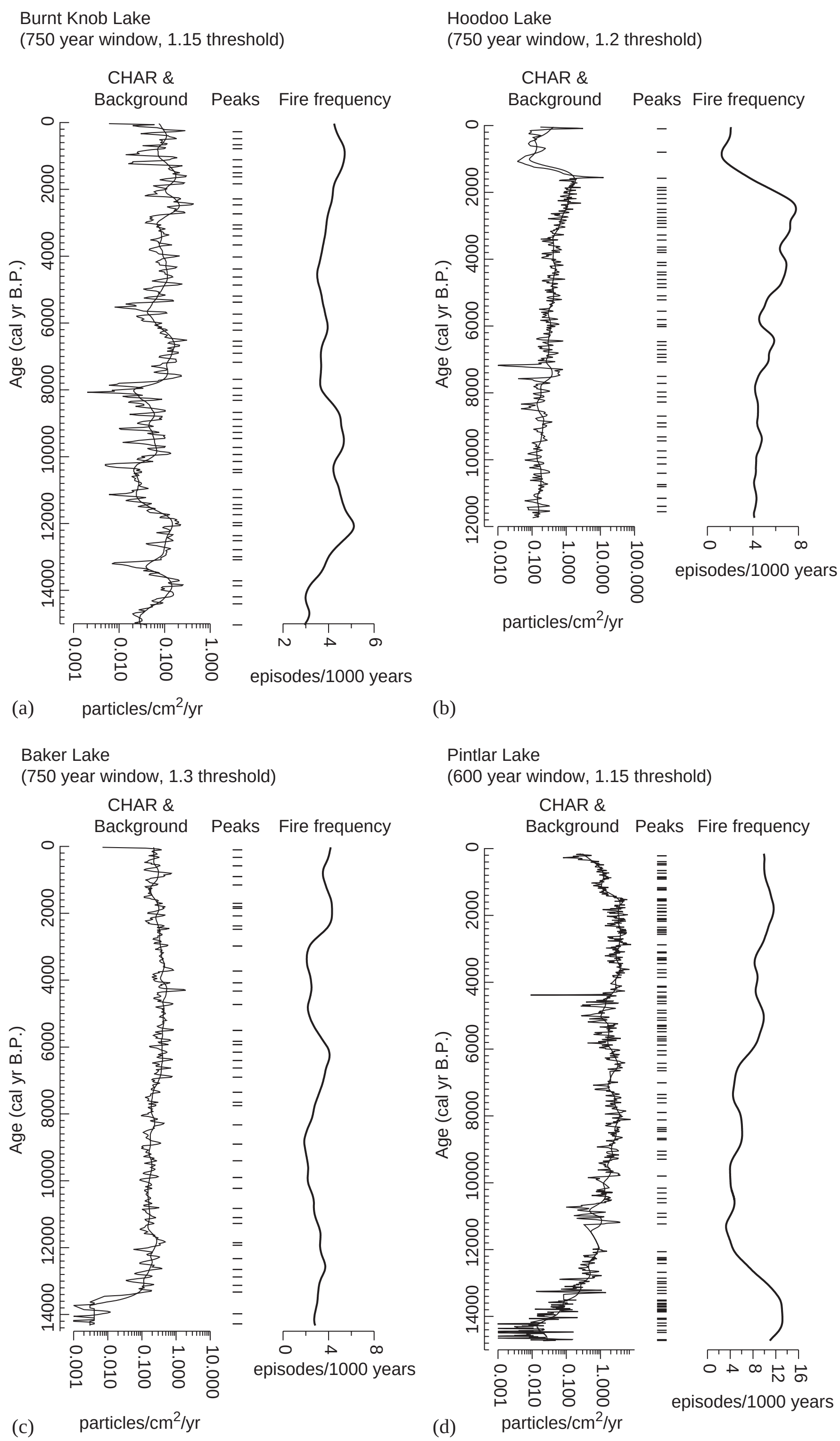

Fig. 6. Decomposition of sedimentary charcoal and fire reconstructions from the study sites. Window width for smoothing background and peak-to-mean threshold ratios are given for each site.

Vegetation and fire reconstructions are also available from Yellowstone National Park (YNP). Cygnet Lake in the central region of YNP lies on the rhyolitic Central Plateau (44.663°N, 110.616°W; 2530 m elevation) (Fig. 1) and is presently summer-dry (Millspaugh et al., 2000). Cygnet Lake is located in *P. contorta* forest. Slough Creek Lake lies in northern YNP (lat 44.918°N, long 110.347°W; 1884 m elevation) (Fig. 1) in

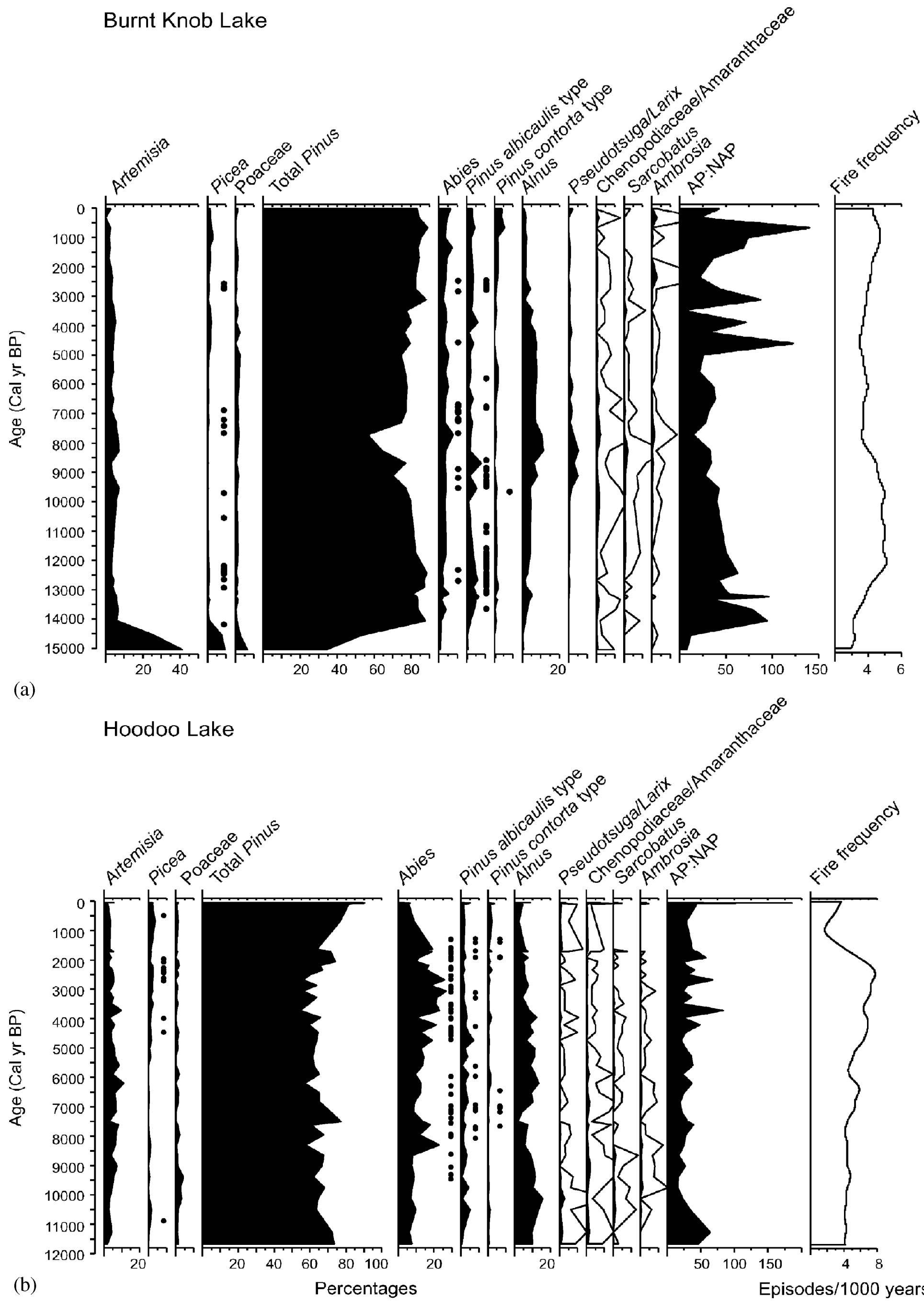

Fig. 7. Pollen diagrams for the study sites. Macrofossils are plotted to right of the appropriate pollen curve, at Baker Lake the lighter dots to the right of the Larix/Pseudotsuga curve represent Larix macrofossils and the darker dots to the left represent Pseudotsuga macrofossils. An open curve to the right of a solid curve represents 10 × exaggeration. Gaps in the fire frequency curve from Pintlar Lake indicate sections of missing core.

a summer-wet region (Millspaugh et al., 2004). Slough Creek Lake is surrounded by *Artemisia* steppe and isolated *Pseudotsuga* stands.

4.2. Late glacial (>11,000 cal yr BP)

The simulations for 14,000 cal yr BP illustrate the response of global and regional climates to the imposition of an ice sheet 60% of its full-glacial size, CO_2 concentration of 230 ppmv (i.e. lower than pre-industrial values), and insolation that was approximately 6% higher in summer and 6% lower in winter than present in the northern hemisphere (Kutzbach et al., 1998) (Table 1). The simulations suggest that winter temperatures in the northern hemisphere were lower than at present and almost as low as at the glacial maximum

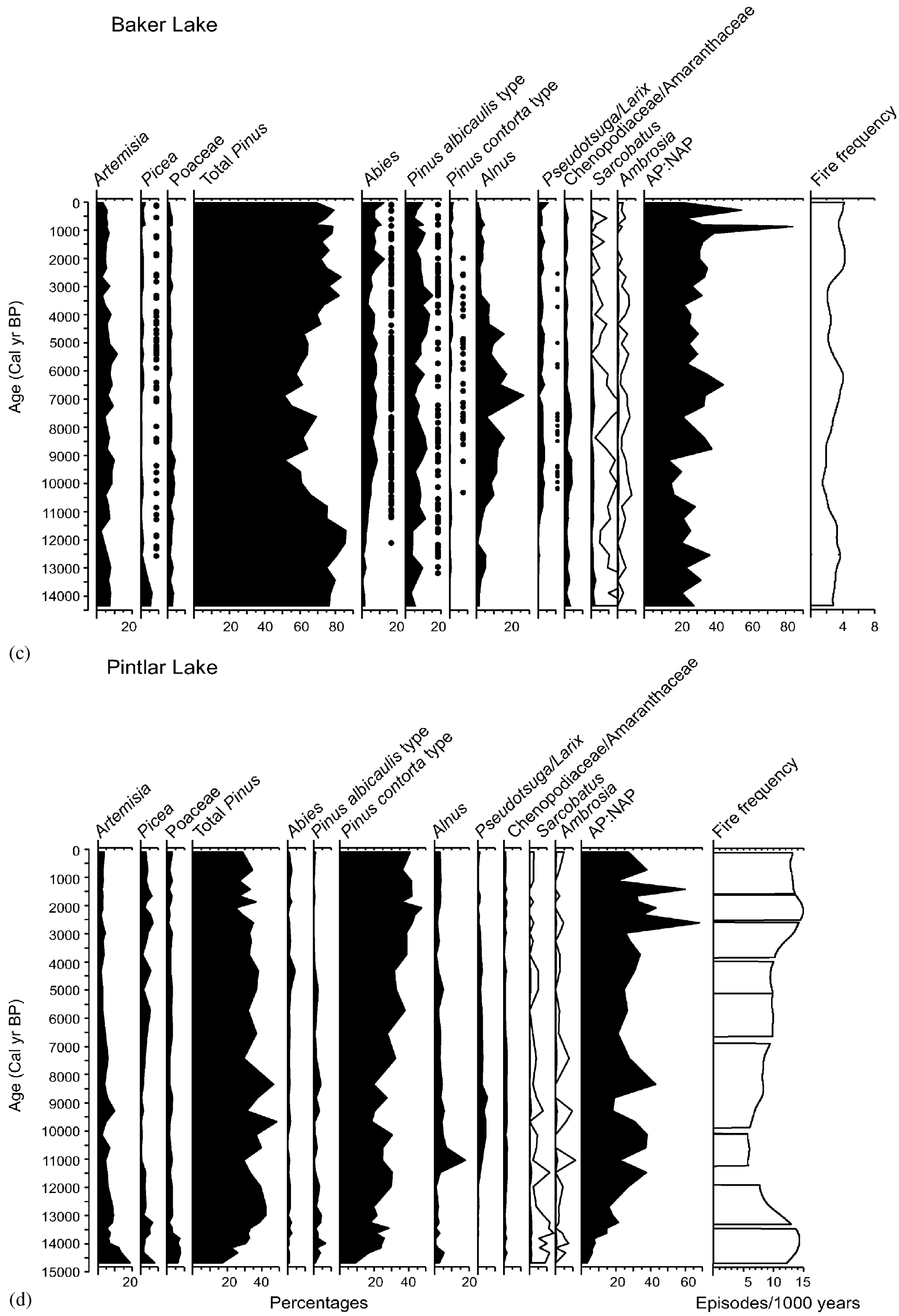

Fig. 7. (*Continued*)

(21,000 cal yr BP). Simulated summer temperatures were similar to those at present but higher than at the glacial maximum as a result of greater summer insolation (Kutzbach et al., 1998). Simulated winters were wetter than present, and summers were generally drier in the western United States, although the coarse resolution of the model (4.4-degrees latitude by 6.5 degrees longitude) limits regionally specific discussion of the simulated precipitation patterns (Bartlein et al. (1998); Kutzbach et al. (1998); see Bartlein and Hostetler (2003) for precipitation anomaly maps for the CCM 1 simulations). Increased winter moisture (relative to earlier) was likely the result of the northward migration of the jet stream from its full-glacial position, as the ice sheet decreased in size and the glacial anticyclone weakened.

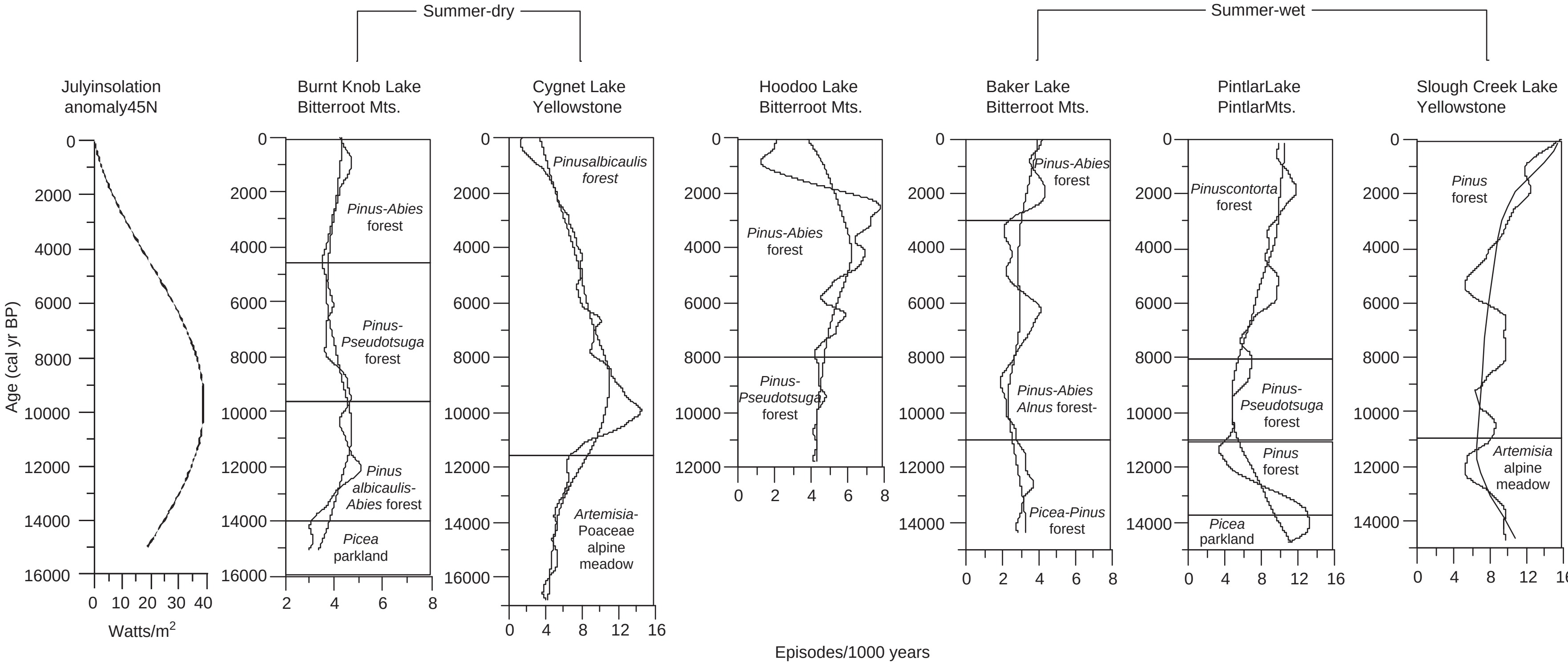

Fig. 8. July insolation anomaly for 45°N latitude and fire frequency for the Northern Rocky Mountain sites. Sites are arranged based on the significance of summer precipitation and summaries of vegetation transitions are indicated for each site. Fire frequency is presented in episodes/1000 years based on the analysis parameters present in Fig. 6, and then also smoothed for each site using a 7500 year window to demonstrate the multi-millennial trends in fire frequency. After ca 8000 cal yr BP, the strong seasonal contrast of precipitation began to attenuate and short-term fluctuations in fire frequency on shorter time scales were not obviously linked to insolation variations on orbital time scales. At the summer-dry sites (Burnt Knob and Cygnet lakes) and also at the transitional site (Hoodoo Lake), fire frequency decreases from the early Holocene to the present, whereas at the summer-wet sites (Baker, Pintlar, and Slough Creek lakes) fire frequency increases to the present.

The paleoecological data from the Bitterroot region are consistent with the model simulations for the northwestern US. Colder-than-present winter conditions are suggested by the presence of *Picea* parkland and alpine vegetation in late-glacial time (Fig. 8). Fire frequency was low at Burnt Knob, Cygnet, Hoodoo, and Baker lakes (in the summer-dry region) during the late-glacial period (Fig. 8), which is consistent with the fire regime in present-day subalpine parkland and alpine environments (Racine et al., 1987; Agee, 1993). Both Pintlar and Slough Creek lakes in the summer-wet region record relatively high fire frequencies (10–12 episodes/1000 years), perhaps reflecting the direct influence of increased summer insolation on surface temperature and soil moisture.

4.3. *Early Holocene (11,000–6800 cal yr BP)*

Simulations for 11,000 cal yr BP illustrate the response to an ice sheet 30% of its full-glacial volume, CO_2 at 267 ppmv (equivalent in these simulations to the pre-industrial value of 280 ppmv, see Kutzbach et al., 1998, for discussion), and summer insolation approximately 8% higher than present in the northern hemisphere (and 8% lower in the winter) (Kutzbach et al., 1998). The simulations show winter conditions that were colder than present and summer conditions that were 2–4 °C warmer than present in the northern hemisphere (Kutzbach et al., 1998) (Table 1). The simulations also show the development of a stronger-than-present (and stronger-than-earlier) northeastern Pacific subtropical high and a deeper-than-present thermal low in the southwestern United States in summer, and a large-scale contrast between lower-than-present precipitation in the Pacific Northwest and higher-than-present precipitation in the southwestern monsoonal region in the model (Bartlein et al., 1998; Kutzbach et al., 1998) (Table 1).

The simulated circulation changes have implications for the pattern of moisture in summer-wet and summer-dry regions of the NRM that can be inferred by examining modern-climate analogues (Mock and Bartlein, 1995; Mock and Brunelle-Daines, 1999). Summer-dry regions should have been drier than present due to the enhanced subtropical high, which at present suppresses precipitation in those regions, whereas summer-wet regions should have been wetter than present due to the enhanced thermal low, which today results in stronger-than-present onshore flow. Whitlock and Bartlein (1993) proposed that the circulation changes associated with increased seasonality of insolation during the early Holocene would intensify modern precipitation regimes but not shift their boundaries, and this hypothesis is supported by fire-frequency data from summer-wet and summer-dry sites in Yellowstone National Park (Millspaugh et al., 2004). If the hypothesis also applies to the NRM, then sites on the western side of the Bitterroot crest (in the summer-dry regime) should have been drier than present during the early to middle Holocene, while sites east of the Bitterroot crest (summer-wet) should have been slightly wetter than present (Table 1).

Fire frequencies at the summer-dry sites (Burnt Knob and Cygnet lakes) were close to their maximum during the early Holocene, consistent with a period of intensified summer drought, low fuel moisture, and frequent dry convective thunderstorms (Figs. 8, 9). Present-day summer-wet sites (Baker, Pintlar, and

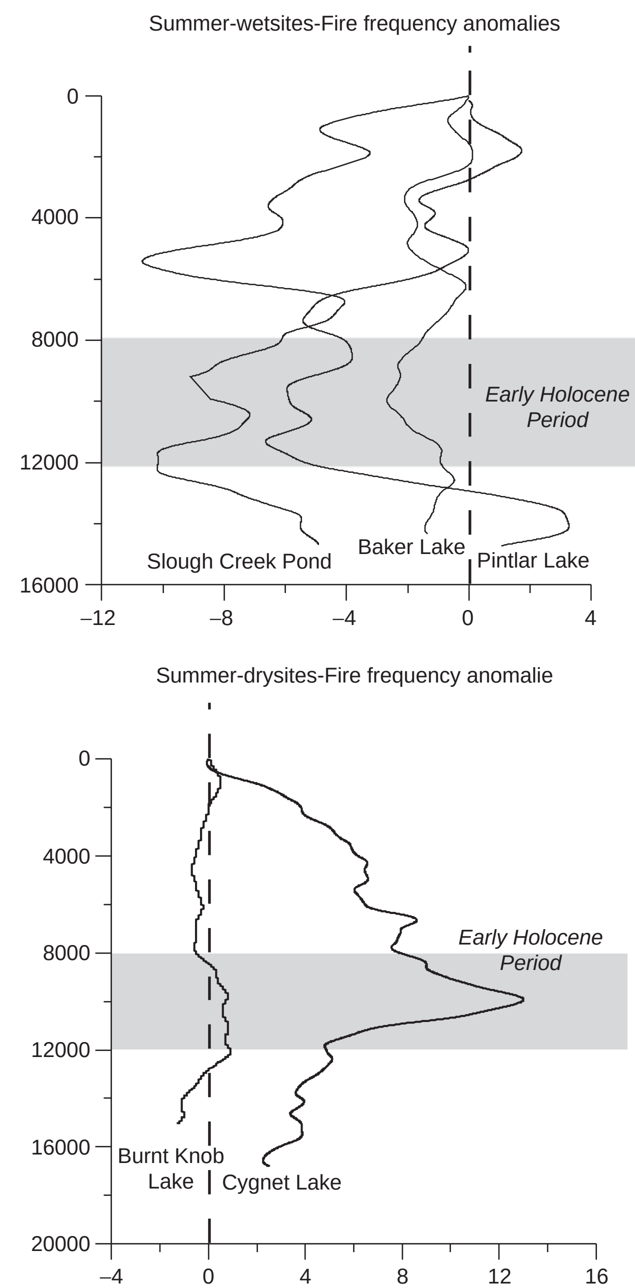

Fig. 9. Fire frequency anomalies for the summer-wet and summer-dry sites. Shading highlights the early Holocene period, note the greatest difference from present occurs during this time interval.

Slough Creek lakes) concurrently showed decreased fire frequency in the early Holocene compared to the previous period and present (Figs. 8, 9), suggesting increased availability of moisture during the fire season. In the summer-wet region, increased moisture availability may have led to a greater incidence of convective thunderstorms (and hence ignitions), but would likely have also led to an increase in fuel moisture.

It is difficult to directly compare the fossil charcoal fire reconstructions with those from tree-rings for the late Holocene, as they are sampled at very different resolutions (annual vs. sub-centennial to millennial). Inspection of Fig. 5 suggests that while there is one period where fires might be considered synchronous across the region, at least at sub-decadal scales (e.g. early 1700s), generally fire events are not occurring in the summer-wet and summer-dry basins during the same years. The nature of the fire regime as well as the sampling design used to reconstruct fire history using tree rings make assessments of synchrony over space tenuous. The watersheds are not adjacent and overall fire frequency is relatively low decreasing the chance that a fire event (or year) would be represented in more than one watershed simply due to the stochastic nature of fire occurrence and behavior. At a finer temporal scale the correspondence between fire events across space may represent the same climatic controls that are recognized over longer time periods during the Holocene but is confounded by the spatial attributes of the tree-ring sampling.

At most sites (Burnt Knob Lake, Mary's Frog Pond, Lost Trail Pass Bog, Pintlar Lake), the pollen data from the early Holocene period indicate the presence of *Pseudotsuga* (Fig. 7). *Pseudotsuga* pollen is common in montane forests in the Rocky Mountains (Fall, 1992; Whitlock, 1993), and its increased presence during the early Holocene suggests warmer conditions than before and an upward shift in upper treeline. The determination that the pollen probably came from *Pseudotsuga* and not *L. lyallii* or *Larix occidentalis* (western larch) is based on two observations. First, *L. lyallii* is a high-elevation species that prefers cool conditions, and taxa associated with the increased occurrence of *Pseudotsuga*/*Larix* pollen during the early Holocene (e.g., Chenopodiaceae/Amaranthaceae type, *Sarcobatus*) (Fig. 8) do not suggest alpine conditions. Second, *L. occidentalis* does not grow near the study sites, whereas *Pseudotsuga* is present in the local or extralocal vegetation at most of the lakes. *Pseudotsuga* pollen was more abundant in the early Holocene at many sites in the Rocky Mountains (Fall, 1992; Thompson et al., 1993; Whitlock, 1993), which is consistent with warmer conditions than before or at present. However the presence of *Larix* (cf. *lyallii*) and *Pseudotsuga* macrofossils throughout the Holocene at Baker Lake suggest both species were present at that site.

4.4. Middle and Late Holocene (6800–0 cal yr BP)

The simulations for 6000 cal yr BP portray the response to an ice sheet near its modern volume, CO_2 concentrations at 267 ppmv, and insolation approximately 6% greater than present during the summer and 6% less than present during the winter in the northern hemisphere (Kutzbach et al., 1998). Simulated winter temperatures were close to modern. Summer temperatures were 1–2 °C higher than in the late-glacial or at present as a result of the still amplified seasonal cycle of insolation (Table 1). Simulations for the western United States for the middle Holocene indicate that the subtropical high was weaker than during the early Holocene, but still stronger than present, as was the thermal low in the southwestern United States.

Recent simulations for 6000 cal yr BP with coupled atmosphere–ocean general circulation models (AOGCMs) (Harrison et al., 2003) show similar responses, with a slight tendency for oceanic feedback to sharpen the Pacific Northwest-Southwest precipitation anomaly contrast. The analysis of these recent simulations also reveals a link among summer precipitation anomalies in the Pacific Northwest (dry), southwestern monsoonal region (wet), and mid-continent (dry) through large-scale atmospheric circulation dynamics (i.e., large-scale vertical motions). This linkage suggests that spatially heterogeneous precipitation anomalies should be evident during the middle Holocene as a result of large-scale circulation controls in western North America.

Because the amplification of the seasonal cycle of insolation was attenuating during the middle and late Holocene, it is expected that fire frequency would decrease at the summer-dry sites as they became wetter, and increase at the summer-wet sites as they became drier. The long-term trends in the NRM data were consistent with this hypothesis. Fire frequency in the middle and late Holocene generally decreased from the earlier period at the summer-dry sites, including Burnt Knob and Cygnet lakes (Fig. 8). As the subtropical high continued to weaken effective moisture at summer-dry sites increased during the fire season. Decreased onshore flow and less summer precipitation increased fire frequencies at summer-wet sites (Baker, Pintlar, and Slough Creek lakes). Suppressed fire activity in the early Holocene may also have promoted vegetation types with greater fuel loads. As these areas became drier in the late Holocene, higher fuel loads would have led to more frequent fires, as evidenced at Baker, Pintlar, and Slough Creek lakes after ca 7000 cal yr BP (Fig. 8).

Although the fire frequency at Cygnet Lake decreased steadily in the middle and late Holocene (Fig. 8), it increased at Burnt Knob Lake at the time of the Medieval Climate Anomaly (MCA) 1050–650 cal yr BP, (Woodhouse and Overpeck, 1998; Crowley, 2000;

Adams, 2003; Bradley et al., 2003). The MCA is not represented by changes in fire frequency at all Bitterroot sites, but several records in the west do suggest dry conditions during this period (e.g. Graumlich, 1991, 1993; Stine, 1994; Brunelle and Anderson, 2003). Summer-wet sites, including Baker, Pintlar, Slough Creek and Hoodoo lakes, show increases in fire frequency prior to the MCA, at ca 2000 cal yr BP. A similar increase is noted at Dog Lake at ca 2000 cal yr BP, in central British Columbia (Hallett and Walker, 2000), where it is associated with a shift from *Picea*/*Abies* to *Pseudotsuga*/*Larix* forest and decreased effective moisture. Pollen data from Bluebird Lake in southern British Columbia also indicated a shift to drier conditions at 2000 cal yr BP (Hebda, 1995). The British Columbia sites lie in a summer-wet region (Figs. 1, 2).

In addition to sharpening the spatial contrasts in summer precipitation and fire regimes, increased seasonality in the early Holocene also affected vegetation composition among the Bitterroot sites. Burnt Knob, Hoodoo, and Pintlar lakes record an increase in the percentages of *Pseudotsuga*–*Larix* type pollen during the early Holocene, which suggests warmer conditions than before or at present (Fig. 8). Baker Lake records a shift in the early Holocene from a *Picea*–*Pinus* forest to a *Pinus*–*Abies*–*Alnus* forest that reflects warming, as well as increased available moisture. The changes in vegetation composition are not synchronous at all sites, but instead seem to reflect a time-transgressive pattern with increasing elevation. For example, *Pseudotsuga*, a lower elevation species is registered later at Burnt Knob Lake than Pintlar Lake as a result of the time it would take to migrate up to the higher elevation.

Western North America is also subject to significant climatic variations on interannual (e.g. Cayan et al., 1999), decadal (e.g. Cayan et al., 1998; Dettinger et al., 2000; Biondi et al., 2001), multidecadal (Gray et al., 2003) and longer time scales, related in general to ocean–atmosphere coupling over the Pacific Ocean, and in specific to ENSO and other "modes" of climate variability. We cannot yet attempt to interpret the paleoenvironmental records from the NRM region in light of these variations, or in light of ENSO in particular for two reasons: (1) Although a general sense has emerged that ENSO-time scale variations (i.e. 2–7 yr) were weaker in the early Holocene than at present, based on both modeling (e.g. Clement et al., 2000; Otto-Bliesner et al., 2003) and paleoenvironmental data (e.g. Rodbell et al., 1999), there is as yet no clear depiction of the specific history of those variations (Friddell et al., 2003; Rodó and Rodriguez-Arias, 2004). (2) The region we emphasize here features nonstationary (or changing) correlations between ENSO-related teleconnection indices (McCabe and Dettinger, 1999; Brown and Comrie, 2004) with inverse correlations between winter precipitation and ENSO (i.e. dry conditions during warm phases) prevailing during the first and last parts of the 20th Century, and no correlation in the middle part of the century. Consequently, there is no way at present to unambiguously link paleoenvironmental variations in the NRM region with ocean–atmosphere interactions that contribute to interannual and longer time scale climatic variations.

5. Conclusions

Paleoecological analyses from a transect of sites in the Bitterroot region provide a way to examine the long-term fire, vegetation, and climate history. The long-term trends in fire occurrence suggest that, during the early Holocene summer insolation maximum, sites west of the Bitterroot crest recorded relatively high fire frequencies, while sites east of the crest recorded relatively low fire frequencies. These results support the original work from Cygnet Lake and Slough Creek Lake in YNP, which demonstrated that increased summer insolation intensified the contrast between modern precipitation regimes during the early Holocene (Millspaugh et al., 2000; Millspaugh et al., 2004). In both YNP and the Bitterroot region, the boundary did not shift because it was constrained by topography. Currently in the Bitterroot region, the gradient in the seasonal distribution of precipitation is subtle (see Table 1), and fire regimes are more similar to each other than at any other time in the Holocene.

Whitlock et al. (2003) also demonstrate that watershed responses to the early Holocene summer insolation maximum are related to the amount of summer precipitation. Sites in the Oregon Coast Range show high fire frequency in the early Holocene, and low fire frequencies in the late Holocene. Summer-dry sites in the Klamath Mountains in California do not demonstrate a fire response to the increased insolation, however there was a marked increase in xerophytic taxa.

In addition to intensifying the gradient in the distribution of summer precipitation, the increased seasonality of the early Holocene also changed the vegetation composition of the Bitterroot sites. Vegetation changes in the series of sites were broadly similar. In the late-glacial period, the sites indicate the presence of open forests dominated by *Picea* and alpine meadow, both of which reflect conditions cooler and drier than present. These open forests were replaced in the early to middle Holocene by more dense forests composed mainly of *Pinus* and *Pseudotsuga* which suggest conditions warmer and/or effectively drier than present. Modern forest composition was established at all sites by ca 3000 cal yr BP. The variations in the timing of the shifts in vegetation are mostly related to the elevation of the site rather than its position along the climatic gradient.

Paleoecology provides insights that may be useful in understanding future changes in climate as a result of increases in greenhouse gases. Climate-model simulations suggest that January and July temperatures will increase by approximately 5 °C in the next 50 years (Shafer et al., 2001). Changes in January precipitation are projected to be spatially heterogeneous with regions east of the Bitterroot crest (summer-wet) remaining similar to present, and some areas west of the crest receiving up to 100 mm more precipitation than at present (Shafer et al., 2001). Information on how past climate change has affected vegetation and fire regimes at local-to-regional scales helps to evaluate the resilience of specific locations to projected changes in future climate. In the Bitterroot region, based on the response of vegetation and fire regimes to past climate changes, we can expect changes in forest composition toward more thermophilous assemblages and fire-adapted communities. Spatially heterogeneous changes in fire frequency are also suggested and may depend on the location of the site along a changing environmental gradient.

Acknowledgments

This manuscript is based largely on the primary author's dissertation research at the University of Oregon. The research was supported by National Science Foundation Grants SBR-9616951, ATM-0117160, ATM-9910638, and a University of Oregon Doctoral Dissertation Research Grant. Many thanks to Todd Daines and Tom Minckley for field assistance, and to Scott Anderson and an anonymous reviewer for their thoughtful suggestions for manuscript improvement.

References

Adams, K., 2003. Age and paleoclimatic significance of late Holocene lakes in Carson Sink, NV, Quaternary Research 60, 294–306.

Agee, J.K., 1993. Fire Ecology of Pacific Northwest Forests. Island Press, Washington, DC, p. 493.

Arno, S. 1979. Forest regions of Montana. USDA Research Paper INT-218.

Barnosky, C.W., Anderson, P.M., Bartlein, P.J., 1987. The northwestern U.S. during deglaciation: vegetational history and paleoclimatic implications. In: Ruddiman, W.F., Wright, H.E. (Eds.), North America and Adjacent Oceans During the Last Deglaciation. The Geology of North America, vol. K-3. Geological Society of America, Boulder, pp. 289–321.

Bartlein, P.J., Hostetler, S.W., 2003. Modeling paleoclimates. In: Gillespie, A., Porter, S.C., Atwater, B. (Eds.), The Quaternary Period in the United States. Elsevier, Amsterdam, pp. 563–582 (Chapter 27).

Bartlein, P.J., Hostetler, S.W., 2004. Modeling paleoclimates. In: Gillespie, A.R., Porter, S.C., Atwater, B.F. (Eds.), The Quaternary Period in the United States. Developments in Quaternary Science. Elsevier, Amsterdam, pp. 563–582.

Bartlein, P.J., Anderson, K.H., Anderson, P.M., Edwards, M.E., Mock, C.J., Thompson, R.S., Webb, R.S., Webb III, T., Whitlock, C., 1998. Paleoclimate simulations for North America over the past 21,000 years: features of the simulation climate and comparisons with paleoenvironmental data. Quaternary Science Reviews 17, 549–585.

Biondi, F., Gershunov, A., Cayan, D.R., 2001. North Pacific decadal climate variability since 1661. Journal of Climate 14, 5–10.

Bradbury, J.P., 1996. Charcoal deposition and redeposition in Elk Lake, Minnesota, USA. The Holocene 3, 339–344.

Bradley, J.P., Hughes, M., Diaz, H.F., 2003. Climate in medieval time. Science 302, 404–405.

Brown, D.P., Comrie, A.C., 2004. A winter precipitation 'dipole' in the western United States associated with multidecadal ENSO variability. Geophysical Research Letters 31, L09203.

Brunelle-Daines, A., 2002. Holocene changes in fire, climate, and vegetation in the Northern Rocky Mountains of Idaho and western Montana. Ph.D. Dissertation, University of Oregon, Eugene, Oregon.

Brunelle, A., Anderson, R.S., 2003. Sedimentary charcoal as an indicator of late-Holocene drought in the Sierra Nevada, California and its relevance to the future. The Holocene 13, 21–28.

Brunelle, A., Whitlock, C., 2003. Postglacial fire, vegetation, and climate history in the clearwater range, Northern Idaho, USA. Quaternary Research 60, 307–318.

Carrara, P.E., Trimble, D.A., 1992. A Glacier Peak and Mount Saint Helens J volcanic ash couplet and the timing of deglaciation in the Colville Valley area, Washington. Canadian Journal of Earth Science 29, 2397–2405.

Cayan, D.R., Dettinger, M.D., Diaz, H.F., Graham, N.E., 1998. Decadal variability of precipitation over Western North America. Journal of Climate 11, 3148–3166.

Cayan, D.R., Redmond, K.T., Riddle, L.B., 1999. ENSO and hydrologic extremes in the western United States. Journal of Climate 12, 2881–2893.

Clark, J.S., 1988. Particle motion and the theory of stratigraphic charcoal analysis: source area, transportation, deposition, and sampling. Quaternary Research 30, 81–91.

Clement, A.C., Seager, R., Cane, M.A., 2000. Suppression of El Niño during the mid-Holocene by changes in the Earth's orbit. Paleoceanography 15, 731–737.

Cleveland, W.S., 1993. Visualizing Data. Hobart Press, 360pp.

Crowley, T.J., 2000. Causes of climate change over the last 1000 years. Science 289, 270–277.

Dean Jr., W.E., 1974. Determination of carbonate and organic matter in calcareous sediments by loss on ignition comparison to other methods. Journal of Sedimentary Petrology 44, 242–248.

Dettinger, M.D., Cayan, D.R., McCabe, G.J., Marengo, J.A., 2000. Multiscale streamflow variability associated with El Niño/Southern Oscillation. In: Diaz, H.F., Markgraf, V. (Eds.), El Niño and the Southern Oscillation: Multiscale Variability and Global and Regional Impacts. Cambridge University Press, Cambridge, UK, pp. 113–147.

Doerner, J.P., Carrara, P.E., 1999. Deglaciation and postglacial vegetation history of the West Mountains, west-central Idaho, USA. Arctic, Antarctic, and Alpine Research 31, 303–311.

Doerner, J.P., Carrara, P.E., 2001. Late Quaternary vegetation and climatic history of the Long Valley area, west-central Idaho, U.S.A. Quaternary Research 56, 103–111.

Faegri, K., Kaland, P.E., Kzywinski, K., 1989. Textbook of Pollen Analysis. Wiley, New York, p. 323.

Fall, P.L., 1992. Spatial patterns of atmospheric pollen dispersal in the Colorado Rocky Mountains, USA. Review of Paleaeobotany and Palynology 74, 293–313.

Fall, P.L., Davis, P.T., Zielinski, G.A., 1995. Late Quaternary vegetation and climate of the Wind River Range, Wyoming. Quaternary Research 43, 393–404.

Finklin, A.I. 1983. Weather and climate of the Selway-Bitterroot Wilderness. Northwest Naturalist Books, Idaho, p. 113.

Friddell, J.E., Thunell, R.C., Guilderson, T.P., Kashgarian, M., 2003. Increased northeast Pacific climatic variability during the warm middle Holocene. Geophysical Research Letters 30 (11) 14-4–14-4.

Gardner, J.J., Whitlock, C., 2001. Charcoal accumulation following a recent fire in the Cascade Range, northwestern USA, and its relevance for fire-history studies. The Holocene 5, 541–549.

Gedye, S.J., Ammann, B., Oldfield, F., Tinner, W., 2000. The use of mineral magnetism in the reconstruction of fire history: a case study from Lago di Origlio, Swiss Alps. Palaeogeography, Palaeoclimatology, Palaeoecology 164, 101–110.

Graumlich, L.J., 1991. Subalpine tree growth, climate, and increasing CO_2: an assessment of recent growth trends. Ecology 72, 1–11.

Graumlich, L.J., 1993. A 1000-year record of temperature and precipitation in the Sierra Nevada. Quaternary Research 39, 249–255.

Gray, S.J., Betancourt, J.L., Fastie, C.L., Jackson, S.T., 2003. Patterns and sources of multidecadal oscillations in drought-sensitive tree-ring records from the central and southern Rocky Mountains. Geophysical Research Letters 30 41-1–49-4.

Hallett, D.J., Walker, R.C., 2000. Paleoecology and its application to fire and vegetation management in Kootenay National Park, British Columbia. Journal of Paleolimnology 24, 401–414.

Harrison, S.P., Kutzbach, J.E., Liu, Z., Bartlein, P.J., Otto-Bliesner, B., Muhs, D., Prentice, I.C., Thompson, R.S., 2003. Mid-Holocene climates of the Americas: a dynamical response to changed seasonality. Climate Dynamics 20, 663–688.

Hebda, R.J., 1995. British Columbia vegetation and climate history with focus on 6 ka B.P. Geographie Physique et Quaternaire 49, 55–79.

Hitchcock, C.L., Cronquist, A., 1973. Flora of the Pacific Northwest: an Illustrated Manual. University of Washington Press, Seattle, Washington.

Hunt, R.S. 1993. Abies. In "Flora of North America North of Mexico. Vol. 2. Pteridophytes and Gymnosperms" (Flora of North America Editorial Committee), pp. 354–362. Oxford University Press, New York.

Kapp, R.O., 1969. How to Know Pollen and Spores. William C. Brown Publishing, Iowa.

Karsian, A.E., 1995. A 6800 year vegetation and fire history in the Bitterroot Mountain Range, Montana. Masters Thesis, University of Montana.

Kipfmueller, K.F., 2003. Fire–climate–vegetation interactions in subalpine forests of the Selway-Bitterroot wilderness area, Idaho and Montana, USA. Ph.D. Dissertation, The University of Arizona, 322pp.

Kutzbach, J., Gallimore, R., Harrison, S., Behling, P., Selin, R., Laarif, F., 1998. Climate and biome simulations for the past 21,000 years. Quaternary Science Reviews 17, 473–506.

Long, C.J., Whitlock, C., Bartlein, P.J., Millspaugh, S.H., 1998. A 9000-year fire history from the Oregon Coast Range, based on a high-resolution charcoal study. Canadian Journal of Forestry 28, 774–787.

McCabe, G.J., Dettinger, M.D., 1999. Decadal variations in the strength of ENSO teleconnections with precipitation in the western United States. International Journal of Climatology 19, 1399–1410.

Mehringer Jr., P.J., Arno, S.F., Peterson, K.L., 1977. Postglacial history of Lost Trail Pass Bog, Bitterroot Mountains, Montana. Arctic and Alpine Research 9, 345–368.

Millspaugh, S.H., Whitlock, C., Bartlein, P.J., 2000. Variations in fire frequency and climate over the past 17 000 yr in central Yellowstone National Park. Geology 28, 211–214.

Millspaugh, S.H., Whitlock, C., Bartlein, P.J., 2004. Postglacial fire, vegetation, and climate history of the Yellowstone-Lamar and Central Plateau provinces, Yellowstone National Park. In: Wallace, L.L. (Ed.), After the Fires; the Ecology of Change in Yellowstone National Park. Yale University Press, New Haven, pp. 10–28.

Mock, C.J., 1996. Climatic controls and spatial variations of precipitation in the Western United States. Journal of Climate 9, 1111–1125.

Mock, C.J., Bartlein, P.J., 1995. Spatial variability of late-Quaternary paleoclimates in the western United States. Quaternary Research 44, 425–433.

Mock, C.J., Brunelle-Daines, A.R., 1999. A modern analogue of western United States summer paleoclimate at 6000 years before present. The Holocene 9, 541–545.

Mohr, J.A., Whitlock, C., Skinner, C.N., 2000. Postglacial vegetation and fire history eastern Klamath Mountains, California, USA. The Holocene 10, 587–601.

Moore, P.D., Webb, J.A., Collinson, M.E., 1991. Pollen Analysis, second ed. Blackwell Scientific Publications, Oxford.

Moulton, G. (Ed.), 1998. The Journals of the Lewis and Clark Expedition. University of Nebraska Press, Lincoln.

Otto-Bliesner, B.L., Shields, C., Brady, E.C., Shin, S.I., Liu, Z., 2003. Modeling El Niño and its tropical teleconnections during the last glacial–interglacial cycle. Geophysical Research Letters 30 CLM 4-1–CLM 4-4.

Palmer, C.L., Parker, W.H., 1991. Phenotypic variation in Yukon populations of subalpine fir. Canadian Journal of Botany 69, 1491–1500.

Racine, C.H., Johnson, L.A., Viereck, L.A., 1987. Patterns of vegetation recovery after tundra fires in northwestern Alaska, U.S.A. Arctic and Alpine Research 19, 461–469.

Rodbell, D.T., et al., 1999. An ~15,000-year record of El Niño-driven alluviation in southwestern Ecuador. Science 283, 516–520.

Rodó, X., Rodriguez-Arias, M.-A., 2004. El Niño-Southern Oscillation: absent in the early Holocene. Journal of Climate 17, 423–426.

Ronda, J.P., 1984. Lewis and Clark Among the Indians. University of Nebraska Press, Lincoln.

Shafer, S.L., Bartlein, P.J., Thompson, R.S., 2001. Potential changes in the distributions of western north America tree and shrub taxa under future climate scenarios. Ecosystems 4, 200–215.

Stine, S., 1994. Extreme and persistent drought in California and Patagonia during medieval time. Nature 369, 546–549.

Stuiver, M., Reimer, P.J., Braziunas, T.F., 1998. High-precision radiocarbon age calibration for terrestrial and marine samples. Radiocarbon 40, 1127–1151.

Tang, M., Reiter, E.R., 1984. Plateau monsoons of the Northern Hemisphere: a comparison between North America and Tibet. Monthly Weather Review 112, 617–637.

Thompson, R., Oldfield, F., 1986. Environmental Magnetism. Allen and Unwin Ltd., London.

Thompson, R.S., Whitlock, C., Bartlein, P.J., Harrison, S.P., Spaulding, G.W., 1993. Climatic changes in Western United States since 18,000 yr BP. In: Wright, Jr., H.E., Kutzbach, J.E., Webb III, T., Ruddiman, W.F., Street-Perrott, F.A. (Eds.), Global climates since the last glacial maximum. University of Minnesota Press, Minneapolis, Minnesota, USA, pp. 468–513.

Troels-Smith, J., 1955. Characterization of unconsolidated sediments: Geological Survey of Denmark, ser. IV, vol. 3, no. 10, 72p.

Whitlock, C., 1993. Postglacial vegetation and climate of Grand Teton and Southern Yellowstone National Parks. Ecological Monographs 63, 173–198.

Whitlock, C., Bartlein, P.J., 1993. Spatial variations of Holocene climatic change in the Yellowstone region. Quaternary Research 39, 231–238.

Whitlock, C., Larsen, C.P.S., 2002. Charcoal as a fire proxy. In: Smol, J.P., Birks, H.J.B, Last, W.M. (Eds.), Tracking Environmental Change Using Lake Sediments: vol. 2. Biological Techniques and Indicators. Kluwer Academic Publishers, Dordrecht, pp. 85–97.

Whitlock, C., Millspaugh, S.H., 1996. Testing the assumptions of fire-history studies: an examination of modern charcoal accumulation in Yellowstone National Park, USA. The Holocene 6, 7–15.

Whitlock, C., Bartlein, P.J., Markgraf, V., Ashworth, A.C., 2001. The midlatitudes of North and South America during the last glacial maximum and early Holocene: similar paleoclimatic sequences despite differing large-scale controls. In: Markgraf, V. (Ed.), Interhemispheric climate linkages. Academic Press, San Diego, pp. 391–416.

Whitlock, C., Shafer, S.L., Marlon, J., 2003. The role of climate and vegetation change in shaping past and future fire regimes in the northwestern US and the implications for ecosystem management Source. Forest Ecology and Management 178, 5–21.

Woodhouse, C.A., Overpeck, J.T., 1998. 2000 years of drought variability in the central United States. Bulletin of American Meteorological Society 79, 2693–2714.

Zdanowicz, C.M., Zielinski, G.A., Germani, M.S., 1999. Mount Mazama eruption: calendrical age verified and atmospheric impact assessed. Geology 27, 621–624.